Surface modified rice husk ceramic particles as a functional additive

Cheng, Lehua; Yu, Dongrui; Hu, Enzhu; Tang, Yuchao; Hu, Kunhong; Dearn, Karl David; Hu, Xianguo; Wang, Min

DOI:
10.5714/CL.2018.26.051
10.5714/CL.2018.26.051

CARBON letters

Original Articles
Carbon Letters Vol. 26, 51-60 (2018)

Surface modified rice husk ceramic particles as a functional additive: Improving the tribological behaviour of aluminium matrix composites

Lehua Cheng[1], Dongrui Yu[2], Enzhu Hu[3,♠], Yuchao Tang[3], Kunhong Hu[3], Karl David Dearn[4,♠], Xianguo Hu[2], and Min Wang[1]

[1]College of Chemical and Materials Engineering, Chaohu University , Hefei, 238000, PR. China
[2]Institute of Tribology, Hefei University of Technology, 193 Tunxi Road, Hefei 230009, PR. China
[3]Department of Chemical and Materials Engineering, Hefei University, 99 Jinxiu Road, Hefei 230601, PR. China;4 Department of Mechanical Engineering, School of Engineering, University of Birmingham, Edgbaston, Birmingham, B15 2TT, United Kingdom

Article Info

Received 8 May 2017
Accepted 12 December 2017

♠Corresponding Author
E-mail: huez@hfuu.edu.cn
huenzhu7@163.com
k.d.dearn@bham.ac.uk
Tel: +86-551-62158439
+44-121-414 4190

Open Access

DOI: http://dx.doi.org/10.5714/CL.2018.26.051

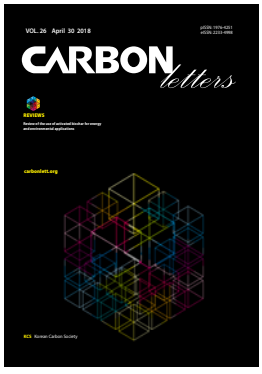

http://carbonlett.org

pISSN: 1976-4251
eISSN: 2233-4998

Abstract

An electroless deposition method was used to modify the surface properties of rice husk ceramic particles (RHC) by depositing nano-nickel on the surface of the RHC (Ni-RHC). The dry tribological performances of aluminum matrix composite adobes containing different contents of RHC and Ni-RHC particles have been investigated using a micro-tribometer. Results showed that the Ni–RHC particles substantially improved both the friction and wear properties of the Ni-RHC/aluminum matrix adobes. The optimal concentration was determined to be 15 wt% for both the RHC and Ni–RHC particles. The improvements in the tribological properties of aluminum adobes including the Ni-RHC were ascribed to friction-induced peeling off of Ni coating and formation of protection layer on the wear zone, both of which led to low friction and wear volume.

Key words: Rice husk, Engineering ceramics, Aluminum-matrix composite, Nickel coating

1. Introduction

Rice husk is a flexible base material that can be used to prepare renewable biomass fuel[1,2], solid fuel[3], white carbon black[4], adsorption materials[5], and many other things. The comprehensive utilization of a wide range of biomass resources continues to receive increasing attention from researchers looking to develop solutions to ongoing global environmental and energy crises [6,7]. China is the world's largest rice-growing country. The annual production of rice has been estimated at up to 180 million tons, which would yield 36 million tons of rice husk. Storing large amounts of rice husk requires considerable space. Burning rice husk, on for example a farm, can result in serious pollution and a large reduction in local air quality. This, therefore, provides a good motivation to develop urgently needed applications and uses for rice husk [8,9]. The preparation of rice husk ceramics can complete the comprehensive utilization of rice husk resources.

At present, due to their high hardness and elastic modulus properties, bio-based ceramic particles can be used in the preparation of wear-resistant materials, such as polymer sliding bearings, and functional additives in lubricating oils. Shibata *et al*. [10] investigated rice bran ceramic (RBC) and glass beads to improve the mechanical and tribological properties of Polyamide (PA66). The wear resistance mechanism of RBC and glass beads is prevention of wear debris forming within wear traces. Shibata *et al*.[11] and Dugarjav *et al*. [12] investigated the sliding of rice husk ceramic (RHC) particle composites against a variety of materials under dry conditions. They indicated that the development of robust transfer films

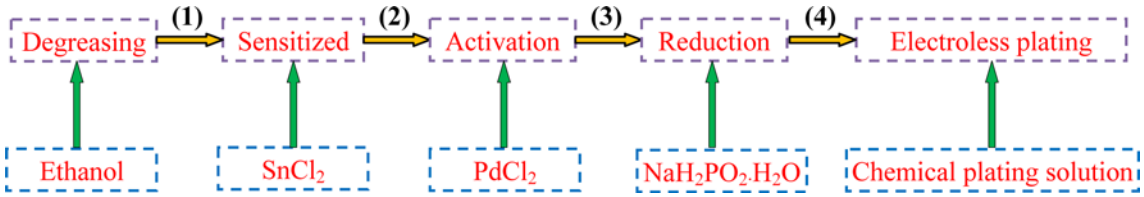

Fig. 1. Preparation processes for Ni-RHC particles

within the wear traces resulted in lower friction coefficients and wear rates. Shibata *et al*. [13] also used RHC particles to prepared pantograph contact strip material (copper/carbon/RBC composite) for railways; the material's tribological behaviors have also been studied. Results have showed that obtained low friction and wear rates were highly dependent on the formation of transfer films. Chand *et al*. [14] used maleic anhydride as a compatibility agent to improve the surface performance of rice husk particles; the end-product was utilized as a filler in polyvinylchloride, showing that surface modified RHC improved the hardness of composites, leading to reduced wear and friction. Akiyama *et al*. [15] used RBC to reinforce PA66, PA11, PBT, POM, and PP. The wear rate and friction coefficient were reduced in all of the tested materials, demonstrating the potential of RBC particles in producing low friction and high wear resistance polymer composite materials, with the key aspect being the compatibility between the filler and the matrix polymer. Hu *et al*. [16] investigated the tribological behaviour of phenol-based RH adobes under dry friction. The wear rate was found to be related to the apparent contact area. They also demonstrated the potential of RHC particles as a functional additive for lubricating oils[17]. Alaneme *et al*. [18, 19] used rice husk ash and silicon carbide particles as fillers in Al–Mg–Si alloy matrix hybrid composites, and studied the corrosion and wear behavior of the composites. Dinaharan *et al*. [20] investigated the effect of rice husk ash on the microstructure and tensile behavior of AA6061 aluminum matrix composites produced using friction stir processing.

Overall, research on RHC particles as a filler used in metal-matrix composites has been limited. A limiting factor for the application of RHC particles in metal-matrix composites is the compatibility between RHC and metal particles such as Fe, Al, Cu, etc. In order to promote the mechanical, dynamic, and tribological properties of metal-matrix composites, surface metallization technology was studied by referring to references[21-26]. However, there is still a need to address the apparent metallic incompatibility between nano-Ni coated RHC and alumina based materials such as alumina based sliding bearings, etc.; one potential solution to this problem is optimization of the dosage of the nickel plating of RHC particles in alumina based composites.

Only a limited number of studies have been reported on the modifying effect of nano-Ni coated RHC particles (Ni–RHC) on the tribological behavior of aluminum matrix RHC composites. This paper presents the results of a study that examined the dry tribological performance of sintered aluminum matrix composite adobes containing RHC and Ni-modified RHC particles at concentrations of 5, 10, 15, and 20 wt%. Tests were conducted using a micro-tribometer under controlled environmental conditions, with results compared to those for unreinforced sintered aluminum adobes. This work can supply a new way to comprehensively utilize rice husk resources, as well as data to develop alumina based materials such as alumina based sliding bearings, etc.

2. Experimental

2.1. Materials and sample preparation

RHC particles were prepared via high temperature carbonization. These were then added to a phenol resin (25 wt%) mixture and stirred using a glass rod for 15 min. The mixture was then transferred to a porcelain crucible, and this was placed in a tube furnace (model OTF-1200X) at 900°C under N_2 atmosphere conditions for 2 h and then cooled at room temperature. The remainder of the powder comprised the RHC particles.

A simple electroless plating deposition process was conducted to prepare the Ni–RHC particles at the optimal conditions of 60 ºC temperature, 180 min time, pH value of 11, and 180 g/L phosphite dosage [21, 27]. A schematic of the processes is shown in Fig. 1. First, RHC particles were washed in ethanol to remove impurities; they were then the sensitized, activated, and reduced using $SnCl_2$ (20 g/L), $PdCl_2$ (1g/L), and $NaH_2PO_2 \cdot H_2O$ (30 g/L). Electroless plating was then applied. The composition of the electro-plating solution is shown in Tab. 1.

The morphology and composition of the Ni–RHC are shown in Fig. 2. The surfaces of the sheet-like RHC particles were coated with copious amounts of Ni particles. Nano measurement software was used to analyze the particle diameter distribution of the Ni particles on the surface of RHC. The analysis process was conducted by choosing Ni particles according to the blue arrow shown in Fig. 2 (b). The average particle diameter (APD) was approximately 84 nm. X-ray diffraction (XRD) analysis indicated that Ni particles (Crystal faces 111 and 200) existed on the surface of RHC, as shown in Fig. 2 (c)

Table 1. Compositions of chemical plating solutions

Items	Chemical formula	Concentration (g/L)
Nickelous sulfate	$NiSO_4 \cdot 6H_2O$	30
Sodium hypophosphite	$NaH_2PO_2 \cdot H_2O$	30
Thiourea	CH_4N_2S	0.001
Trisodium citrate dihydrate	$Na_3C_6H_5O_7 \cdot 2H_2O$	25
Ammonium chloride	NH_4Cl	20

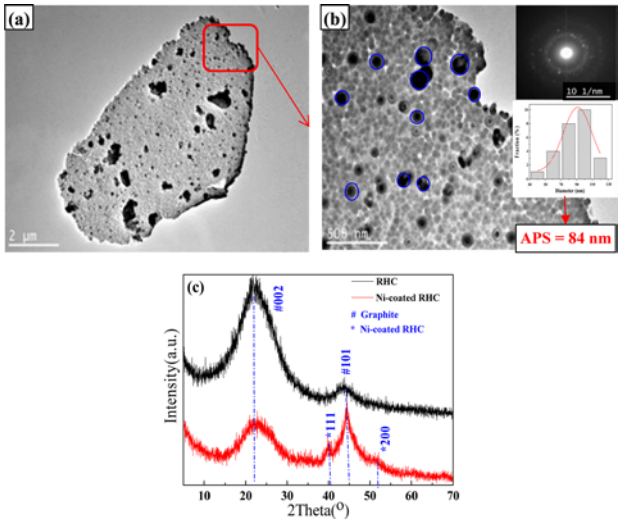

Fig. 2. HRTEM and selected area electron diffraction diagrams (SAED) of Ni-RHC particles.
(a) HRTEM mages of Ni-coated RHC (b) Magnified HRTEM and ASED images (c) XRD image of RHC and Ni-coated RHC

The magnified images of Ni–RHC provided in Fig. 3 show that Ni particles are predominately spherical and have adhered to the surface of the RHC particles. Fig. 3(e) confirms the presence of elemental Ni. The XRF (X-Ray Fluorescence Spectroscopy, PANalytical, Netherlands) analysis shows that the weight ratio of Ni to RHC is 1: 2.25.

A commercially available aluminum powder (Al powder size of 100 μ/nm) was purchased from Qinghe Boxin Wear-resistant Alloy Co. Ltd, China. The test samples were prepared by first preparing a green compact and then sintering. Both RHC and modified Ni–RHC particles were added to the Al powder at concentrations of 1 wt%, 5 wt%, 10 wt%, 15 wt%, and 20 wt% mass percentage. Finally, 5 wt% phenolic resin (PR) was added to the mixture to uniformly disperse the RHC/ Ni–RHC particles in Al powder. Fig. 4 shows the preparation process for the test adobes.

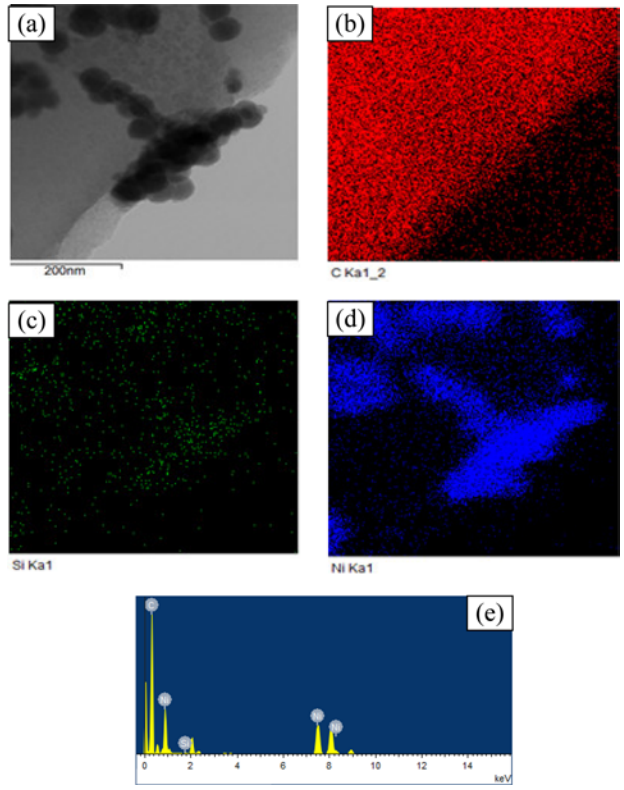

Fig. 3. Element distribution and EDS analysis of selected zones of Ni–RHC particles
(a) SEM images (b) C (c) Si (d) Ni

2.2. Analysis methods

The tribological behavior of the composite adobes was assessed using a micro-tribometer under a controlled atmosphere at 1 N load and 300 rpm speed for 30 min. The test temperature was approximately 25°C and relative humidity

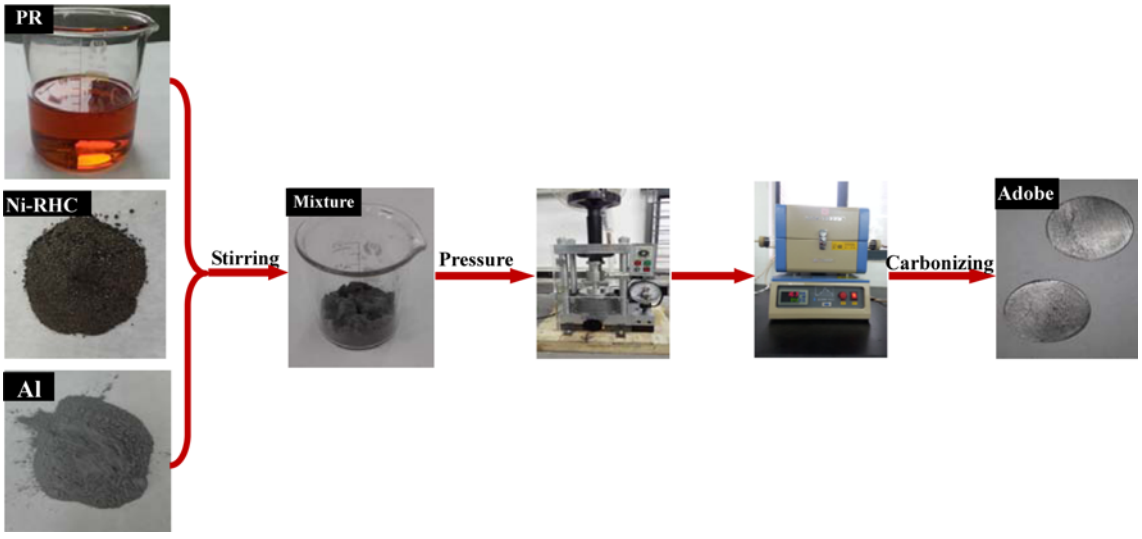

Fig. 4. Preparation process for the composition material adobes

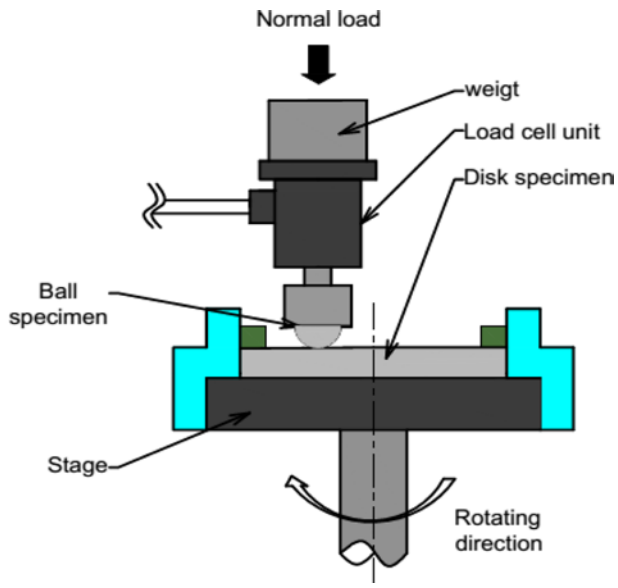

Fig. 5. Schematic diagram of the ball–basic tribometer

was approximately 60% (RH). A schematic of the tribometer is shown in Fig. 5. The upper specimen was a 5 mm diameter stainless-steel (grade 304) ball with a surface roughness of 0.35 μm (Ra) and a hardness of 74.0 (HRA). The lower samples were composite adobes, which were polished with 800-mesh abrasive paper to obtain a similar surface roughness. After testing, the worn traces were investigated using 3D laser scanning microscopy (mode VK-X100K). Each tribological test was conducted three times to reduce experimental deviation. The hardness of the samples was tested using a microindentation and Macro/Vickers hardness testing system (model HV-1000IS). The morphology and compositions of the transfer films on the upper samples were measured and analyzed using SEM/EDS. Using the measured wear track, and according to the formulas, wear resistance of the composite materials was calculated according to the wear volume and the apparent contact area (S_a, mm^2) [16]:

$$V=2\pi RS_c \quad (1)$$

$$S_a=\pi(R+d/2)^2-\pi(R-d/2)^2=2\pi Rd \quad (2)$$

Note: V is wear volume of disk sample; S_c is cross-sectional area of wear trace; R is the upper specimen radius (5 mm); and *d* is the wear trace width (μm, WTD), as shown in Figure 8

3. Results

3.1. Friction reduction

Fig. 6 shows the variation in the friction coefficient with various concentrations of RHC and Ni–RHC particles in the aluminum matrix composites adobes. In Fig. 6(a) the friction coefficient of the RHC composites is shown to decrease up to concentrations of 15 wt%, representing a saturation point beyond which the measured friction rises to 20 wt%.The modified Ni–RHC composites showed similar trends, as shown in Fig. 6(b); however the equivalent friction coefficients were all lower than the equivalent RHC concentrations.

3.2. Wear resistance

Fig. 7 shows the wear volume of the aluminum composite adobes with varying concentrations of RHC and Ni–RHC particles. The worn volume of unreinforced aluminum adobe was 0.76 mm^3. With the addition of 5 wt% RHC, the wear volume increased to 0.92 mm^3. Interestingly, beyond this concentration the wear volume decreased continuously, to 0.71 mm^3 at 10 wt% and 0.29 mm^3 at 15 wt% RHC, decreases of 6% and 61%, respectively. For the modified Ni–RHC wear volumes, compared to those of unreinforced aluminum, all decreased with the addition of Ni–RHC to the aluminum composite adobes. This indicates that the modification of RHC with Ni strengthens the wear resistance of the composites [25]. The optimal concentration of Ni–RHC in the aluminum matrix was 15 wt%, which was similar to the case of unmodified RHC addition to aluminum.

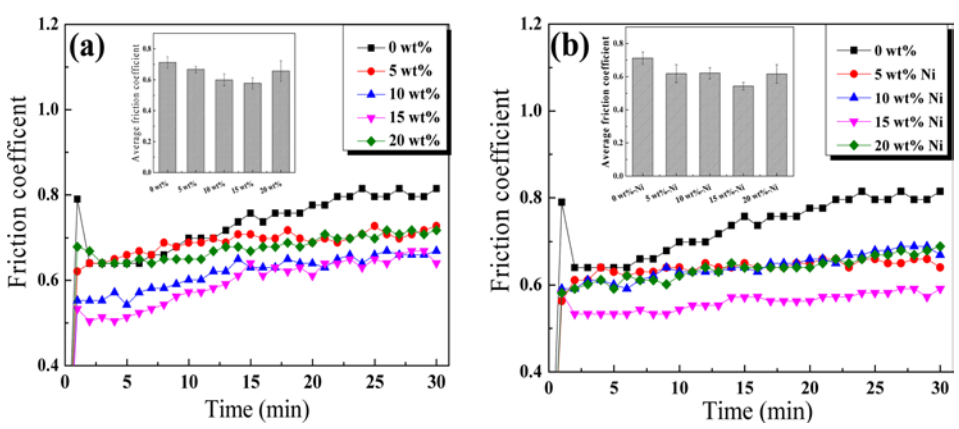

Fig. 6. Variation in friction coefficient with different amounts of RHC or Ni–RHC particles in aluminum-based composite adobes at 1 N and 300 rpm for 30 min: (a) RHC and (b) Ni–RHC

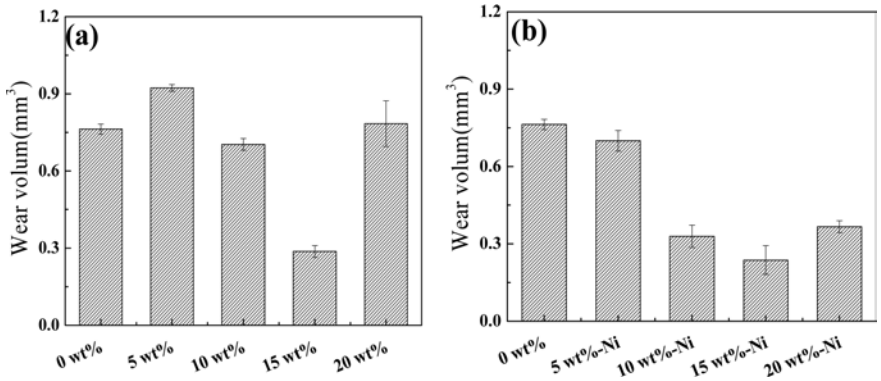

Fig. 7. Variation in wear volume with the addition of RHC or Ni–RHC particles at different amounts in composition material adobes at 1 N and 300 rpm for 30 min: (a) RHC and (b) Ni–RHC

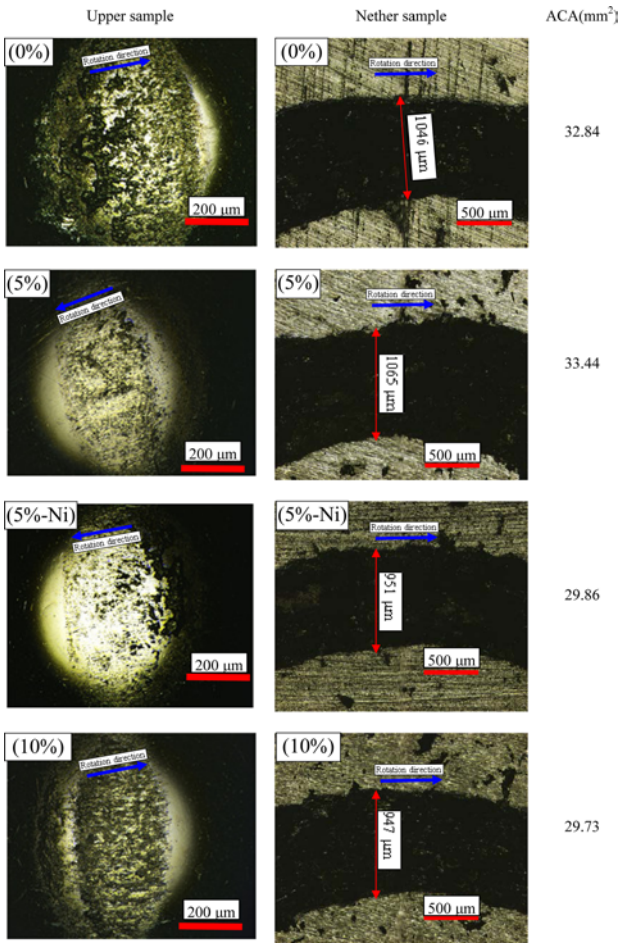

Fig. 8. Optical microscopy images of the upper and nether samples after friction

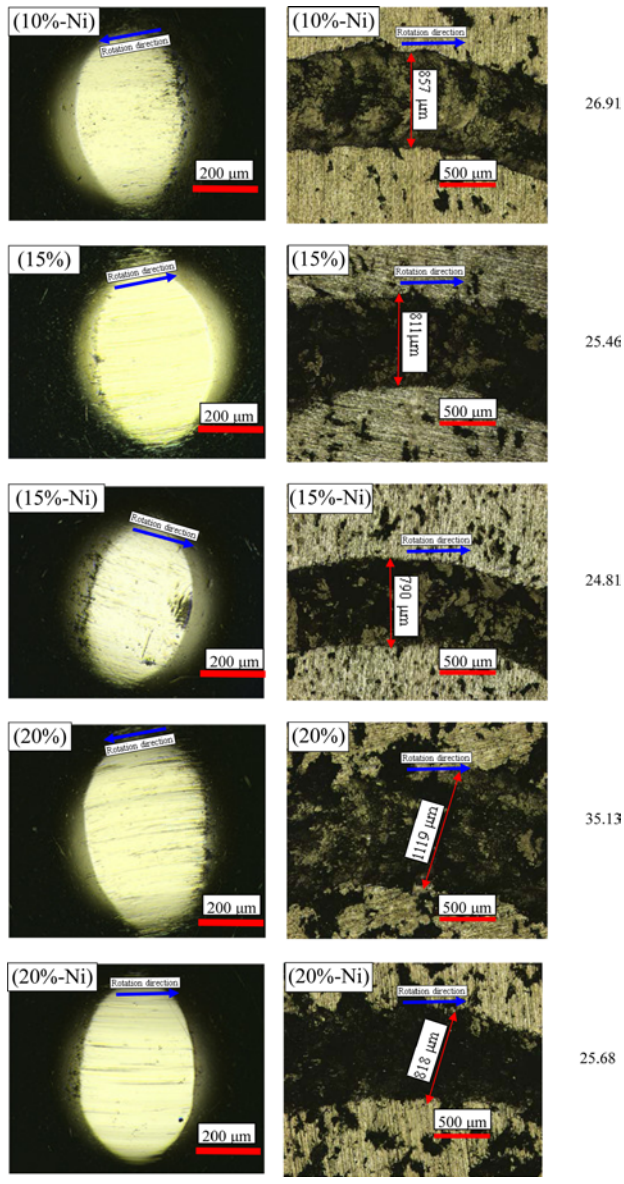

Fig. 8. Continued

3.3. Surface analysis

Fig. 8 shows the morphologies of wear traces for the upper and lower samples after friction. For the unreinforced aluminum adobe, there was clear evidence of a significant transfer

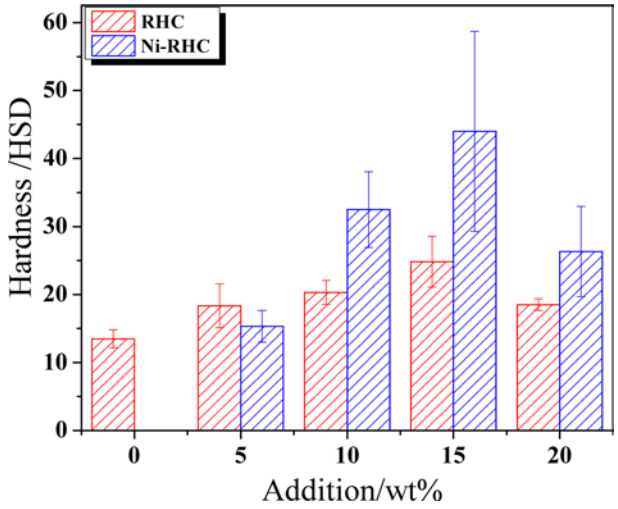

Fig. 9. Hardness of samples with different added amounts of Ni–RHC particles

of wear debris from the aluminum adobes that had adhered to the surface of the stainless steel ball. This phenomenon was ascribed to the greater hardness of steel balls than that of unreinforced aluminum adobe. A similar behavior was also observed on the surface of the abodes with 5 wt% and 10 wt% RHC particulates. However, wear debris decreased significantly with increasing particle concentration, especially with the 15 wt% and 20 wt% RHC composites. For these samples, wear debris was very low, taking a form of scratching and by definition confirming that the hardness of the aluminum composite samples increased with increasing RHC particle concentration.

The wear trace width (WTD) and apparent contact area (ACA) of the unreinforced aluminum adobe were approximately 1046 μm and 32.84 mm^2, respectively. The WTD and ACA values of the adobes with 5, 10, and 15 wt% RHC particles added were 1065 μm and 33.44 mm^2, 947 μm and 29.73 mm^2, and 811 μm and 25.46 mm^2, respectively. In view of the results above, the addition of 15 wt% RHC particles was determined as the optimal concentration, offering minimal values of WTD and ACA. For the modified Ni–RHC particles, the WTD and ACA values of the composite adobes were 951 μm and 29.86 mm^2 (5 wt%), 857 μm and 26.91 mm^2 (10 wt%), and 790 μm and 24.81 mm^2 (15 wt%), representing decreases of 9%, 18%, and 24.5%, respectively, as compared with those of unreinforced aluminum adobes. The optimal concentration was once again determined to be 15 wt % of Ni–RHC particles in the aluminum adobes. Interestingly, the WTD and ACA values both increased with the addition of 20 wt% RHC and Ni–RHC particles to the aluminum powder. The high content Ni-RHC (20 wt%) plays an opposite role in strengthening the hardness, resulting in friable composite materials. These results can be confirmed by the variation in hardness for each sample with different added amounts of RHC or Ni–RHC particles, the details of which can be seen in Fig. 9. The hardness of the composite including 15 wt% Ni-RHC was obviously higher than the hardness of the 20 wt% Ni-RHC composite.

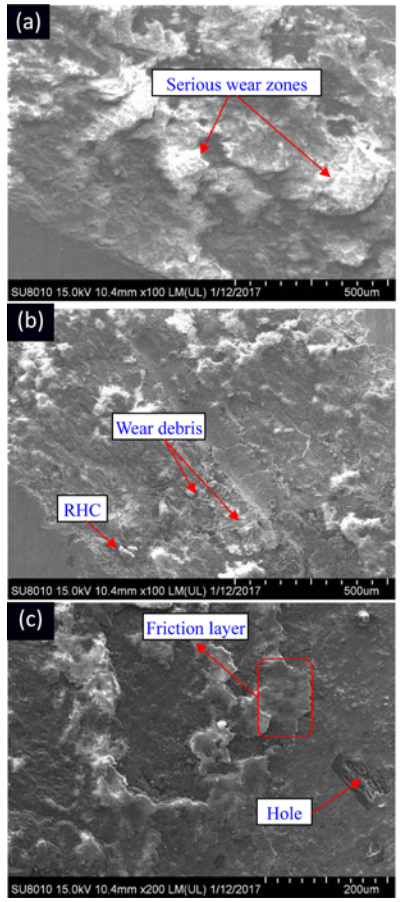

Element	Wear zone
C	6.20
O	53.84
Al	39.96
Si	-

Element	Wear zone
C	17.98
O	34.78
Al	46.48
Si	0.75

Element	Wear zone
C	16.16
O	35.91
Al	41.17
Si	1.60
P	0.61
Fe	2.62
Ni	1.91

Fig. 10. SEM/EDS analysis of wear zones on lower samples (a) 0 wt% RHC/Al (b) 15 wt% RHC/Al (c) 15% Ni-RHC/Al

Fig. 10 shows the variation of surface morphologies of wear traces for lower different samples. Serious wear zones can be observed in Fig. 10(a); these were ascribed to low hardness and lots of wear debris on the wear traces. The wear phenomenon was alleviated via addition of 15 wt% RHC particles; however, lots of wear debris and RHC particles were exfoliated from the sample surface, as shown by the red arrows in Fig. 10(b). Interestingly, friction layers were observed on the wear zones, as shown by the red rectangle in Fig. 10(c); these layers can increase the load capacity of the composites, resulting in lower friction coefficient and wear volume.

Fig. 11 shows the variations in elemental content of the transfer films detected on the various stainless steel upper samples. Interestingly, the transfer films were clearly visible on the surfaces of the samples that had run against the unreinforced aluminum adobe, as they were too on the samples with additions of 15 wt% RHC and 15 wt% Ni-RHC particles, as shown in Figs. 11(a), 11(b) and (c). The EDS spectral analysis indicates that the Ni–RHC particles promoted the formation of transfer film, with elemental Ni detected throughout the contact surface of the stainless steel balls. The elemental Ni content of the sample from the 15 wt% Ni–RHC tests was 0.33 wt%, as shown

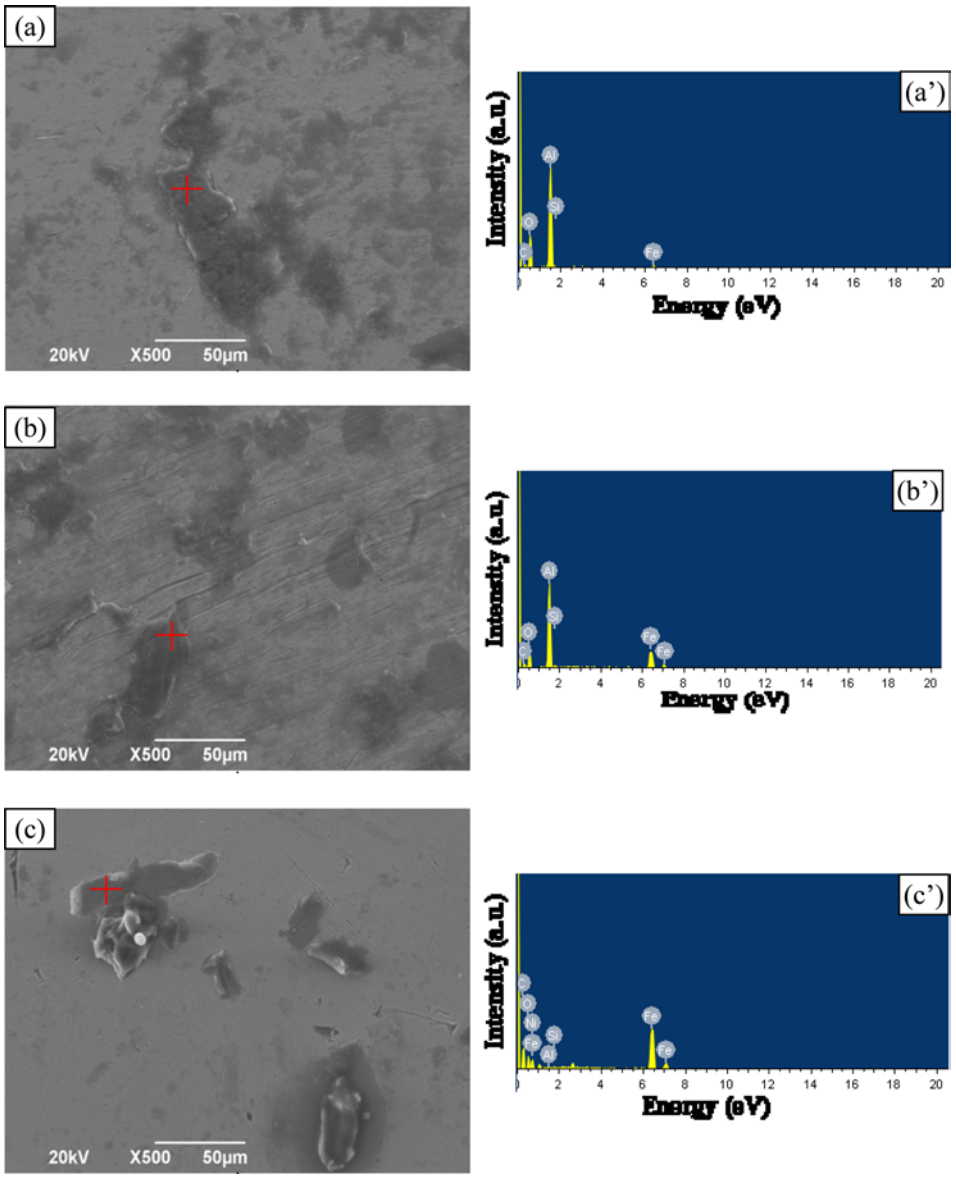

Fig. 11. SEM/EDS analysis of wear zones of steel ball for different samples
(a) and (a') Unreinforced Al, (b) and (b') Al+15 wt% RHC, (c) and (c') Al+15 wt% Ni–RHC

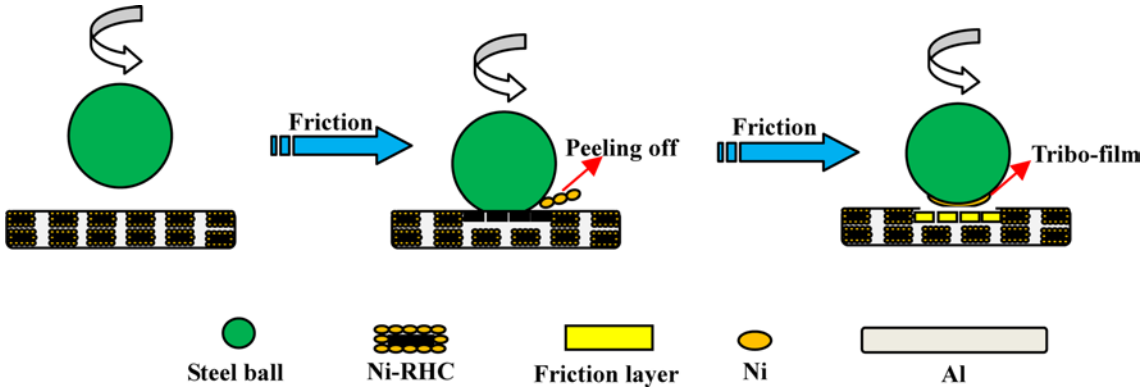

Fig. 12. Schematic diagram of friction and wear mechanism of Ni-RHC particles

Table 2. EDS analysis of wear zones of steel balls for different samples

Items	Element content (wt%)							
	C	O	Al	Fe	Si	Ni	S	Mo
Unreinforced Al	1.91	46.05	46.24	5.32	0.48	-	-	-
Al+ 15 wt% RHC	2.21	23.04	39.32	33.43	2.02	-	-	-
Al+15wt% RHC-Ni	6.65	13.76	0.07	78.45	0.75	0.33	-	-

in Tab. 2. Such a film and friction layer on the lower sample could be used to explain both the low friction coefficient and the wear volume for addition of 15 wt% Ni-RHC to alumina based materials[29].

4. Discussion

The hardness of unreinforced aluminum adobe was significantly lower than that of stainless steel balls, which resulted in the formation of wear products as a film on the surfaces of the steel balls, as shown in Fig. 11(a) and Fig. 8. Despite the presence of wear products transferred to the surface of the wear zone on the steel balls, the changes of friction form and hardness of material [30] led to a low friction coefficient and wear volume, which can be proved by the variation of friction coefficients at the different concentrations of RHC and Ni-RHC.

In general, the addition of functional ceramic particles to metal matrix composites must be done at an optimum dosage. At concentrations of 5 wt% RHC, the friction reduction and wear resistance properties, however, did not improve; this can possibly be ascribed to the RHC particles peeling off from the matrix and those products of the wear process not being of sufficient concentration to provide a sufficiently lubricious film or friction protected layer, resulting in serious wear. Regarding the 5 wt% Ni-RHC, the friction and wear resistance were modified compared to those characteristics of the sample with addition of 5 wt% RHC and pure aluminum material. The phenomenon indicates that the Ni-coating played important roles of anti-friction and anti-wear[31]. The friction reduction and wear resistance properties were obviously modified when 10 wt% and 15 wt% RHC particles were added to the composite materials. The main reason was thought to be friction, which induced lots of RHC particles to peel off, resulting in the sliding friction form changing into a rolling friction form. As for the 10 wt% and 15 wt% Ni-RHC samples, the friction reduction and wear resistance properties were also obviously modified; this was ascribed to the Ni coating, transferred onto the surface of the steel balls, resulting in the formation of a tribo-film and a friction protected layer on the lower sample, as shown in Fig. 10(c) and Fig. 11(c). With increasing addition of RHC and Ni-RHC particles up to 20 wt%, wear resistance properties become worse; this was ascribed to the decrease of the hardness or the density of the materials [32]. The optimum concentration of RHC and Ni–RHC particles in aluminum was 15 wt%. The mechanism of the anti-friction and anti-wear properties of Ni–RHC particles is described in Fig. 12.

Overall, Ni-RHC particles first form a protective layer on the surface of the sample during the friction process. Then, spherical-like Ni is liberated from the RHC particles on the surface of the adobe with friction time extending. Ni along with some of the aluminum matrix formed a transfer film on the surface of the stainless steel balls, resulting in a low friction coefficient. These results suggest that Ni-modified RHC particles can be used as an additive to enhance the friction reduction and wear resistance properties of aluminum matrix composites. The efficacy of the additive is determined by the concentration of Ni–RHC added to the matrix; this concentration controls the hardness of the composite material.

5. Conclusions

The dry tribological performance of sintered aluminum matrix composite adobes containing RHC and Ni-modified RHC particles at concentrations of 5, 10, 15, and 20 wt% has been investigated. Using a micro-tribometer, tests were conducted under controlled environmental conditions, with results compared to those for unreinforced sintered aluminum adobes. The following conclusions are drawn from this study:

Addition of RHC and Ni–RHC particles reduced friction and increased the wear resistance of the aluminum matrix composite adobes.

Compared to the unreinforced samples, induced friction coefficient and generated wear volume were the same, decreasing with increasing concentrations of RHC or Ni–RHC particles to 15 wt%. Beyond this point, at 20 wt%, both friction and wear increased.

The hardness of aluminum matrix composite adobes was determined by the concentration of RHC and Ni–RHC particles, resulting in contrasting tribological performances. The nano-Ni coated RHC can form a friction protected layer; also, friction induced wear caused Ni coating to be 'peeled' off from the RHC particles, forming a transfer film on the surface of the stainless steel counterface, and resulting in low friction coefficient and wear volume.

Both RHC and Ni–RHC particles can be used as functional additives in the development of aluminum-matrix composite bearing materials.

Acknowledgements

The authors wish to express their thanks to Mrs. Yueru Liu and Mr. Xianquan Chao for their assistance with the SEM/EDS and HRTEM tests. Financial support from the National Natural Science Foundation of China (Grant No. 51505121), Anhui Pro-

vincial Natural Science Foundation (Grant Nos.1608085QE119 and 1508085J10) and Natural Science Foundation Project of Anhui Education Committee (KJ2016A503) is gratefully acknowledged. Some of the experimental equipment used in this research, within the Birmingham Centre for Cryogenic Energy Storage, was obtained with support from the Engineering and Physical Sciences Research Council, under the Eight Great Technologies: Energy Storage Theme (grant number EP/L017725/1).

References

[1] Ikura M, Stanciulescu M, Hogan E. Emulsification of pyrolysis derived bio-oil in diesel fuel, Biomass Bioenergy, 24, 221 (2003). https://doi.org/10.1016/S0961-9534(02)00131-9.

[2] Fan X, Zhu JL, Zheng AL, Wei XY, Zhao YP, Cao JP, Zhao W, Lu Y, Chen L, You CY. Rapid characterization of heteroatomic molecules in a bio-oil from pyrolysis of rice husk using atmospheric solids analysis probe mass spectrometry, J. Anal. Appl. Pyrolysis, 115, 16 (2015). https://doi.org/10.1016/j.jaap.2015.06.012.

[3] Wu HC, Ku Y, Tsai HH, Kuo YL, Tseng YH. Rice husk as solid fuel for chemical looping combustion in an annular dual-tube moving bed reactor, Chem. Eng. J., 280, 82 (2015) . https://doi.org/10.1016/j.cej.2015.05.116.

[4] Wang L, Wang X, Zou B, Ma X, Qu Y, Rong C, Li Y, Su Y, Wang Z. Preparation of carbon black from rice husk by hydrolysis, carbonization and pyrolysis, Bioreso.Technol., 102, 8220 (2011). https://doi.org/10.1016/j.biortech.2011.05.079.

[5] Rangabhashiyam S, Anu N, Selvaraju N. Sequestration of dye from textile industry wastewater using agricultural waste products as adsorbents, J. Environ. Chem. Eng., 1, 629 (2013). https://doi.org/10.1016/j.jece.2013.07.014.

[6] Soltani N, Bahrami A, Pech-Canul MI, González LA. Review on the physicochemical treatments of rice husk for production of advanced materials, Chem. Eng. J., 264, 899 (2015). https://doi.org/10.1016/j.cej.2014.11.056.

[7] Asim N., Emdadi Z., Mohammad M., Yarmo MA, Sopian K., Agricultural solid wastes for green desiccant applications: an overview of research achievements, opportunities and perspectives, J. Clean. Prod., 91, 26(2015). https://doi.org/10.1016/j.jclepro.2014.12.015.

[8] Jenkins BM, Global Agriculture: Industrial feedstocks for energy and materials, Encyclopedia of Agriculture and Food Systems, Academic Press, Oxford, 461 (2014). https://doi.org/10.1016/B978-0-444-52512-3.00156-X.

[9] Li Y, Ding X, Guo Y, Rong C, Wang L, Qu Y, Ma X, Wang Z, A new method of comprehensive utilization of rice husk, J. Hazard. Mater., 186, 2151 (2011). http://trove.nla.gov.au/version/164784806.

[10] Shibata K, Yamaguchi T, Hokkirigawa K, Tribological behavior of RH ceramics made from rice husk sliding against stainless steel, alumina, silicon carbide, and silicon nitride, Tribol. Int., 73, 187 (2014). https://doi.org/10.1016/j.triboint.2014.01.021.

[11] Shibata K, Yamaguchi T, Hokkirigawa K. Tribological behavior of polyamide 66/rice bran ceramics and polyamide 66/glass bead composites, Wear, 317, 1 (2014) . https://doi.org/10.1016/j.wear.2014.04.019.

[12] Dugarjav T, Yamaguchi T, Shibata K, Hokkirigawa K. Friction and wear properties of rice husk ceramics under dry condition, J. Mech. Sci. Technol., 24, 85 (2010). DOI: 10.1007/s12206-009-1167-9.

[13] Shibata K, Yamaguchi T, Urabe T, Hokkirigawa K. Experimental study on microscopic wear mechanism of copper/carbon/rice bran ceramics composites, Wear, 294-295, 270 (2012). https://doi.org/10.1016/j.wear.2012.07.004.

[14] Chand N, Sharma P, Fahim M. Tribology of maleic anhydride modified rice-husk filled polyvinylchloride, Wear, 269, 847 (2010). https://doi.org/10.1016/j.wear.2010.08.014.

[15] Akiyama M, Yamaguchi T, Matsumoto K., Hokkirigawa K. Friction and wear of polyamide 66 composites filled with RB ceramics particles under dry condition, Tribol. Online, 5, 87 (2010). https://doi.org/10.2474/trol.5.87.

[16] Hu E, Hu K, Xu Z, Hu X, Dearn KD, Xu Y, Xu Y, Xu L. Investigation into the morphology, composition, structure and dry tribological behavior of rice husk ceramic particles, Appl. Surf. Sci., 366C, 372 (2016). https://doi.org/10.1016/j.apsusc.2016.01.116.

[17] Hu E, Hu K, Dearn KD, Hu X, Xu Y, Yu D, Gu H, Tang Y. Tribological performance of rice husk ceramic particles as a solid additive in liquid paraffin, Tribol. Int., 103, 139 (2016). https://doi.org/10.1016/j.triboint.2016.06.035.

[18] Alanemea KK, Adewaleb TM, Olubambic PA. Corrosion and wear behaviour of Al–Mg–Si alloy matrix hybrid composites reinforced with rice husk ash and silicon carbide. J. Mater. Res. Technol., 3, 9 (2014). https://doi.org/10.1016/j.jmrt.2013.10.008.

[19] Alanemea KK, Olubambic PA. Corrosion and wear behaviour of rice husk ash—Alumina reinforced Al–Mg–Si alloy matrix hybrid composites. J. Mater. Res. Technol., 2, 188 (2013). https://doi.org/10.1016/j.jmrt.2013.02.005.

[20] Dinaharana I, Kalaiselvanb K, Muruganc N. Influence of rice husk ash particles on microstructure and tensile behavior of AA6061 aluminum matrix composites produced using friction stir processing. Compos. Commu., 3, 42 (2017). https://doi.org/10.1016/j.coco.2017.02.001.

[21] Bhav Singh B, Balasubramanian M.. Processing and properties of copper-coated carbon fibre reinforced aluminium alloy composites, J. Mater. Process. Technol., 209, 2104 (2009). https://doi.org/10.1016/j.jmatprotec.2008.05.002.

[22] Zhang Q, Wu M, Zhao W. Electroless nickel plating on hollow glass microspheres, Surf. Coat.Technol., 192, 213 (2005). https://doi.org/10.1016/j.surfcoat.2004.06.013.

[23] Wang LY, Tu JP, Chen WX, Wang YC, Liu XK, Olk C, Cheng DH, Zhang XB. Friction and wear behavior of electroless Ni-based CNT composite coatings, Wear, 254, 1289 (2003). https://doi.org/10.1016/S0043-1648(03)00171-6.

[24] Chen Y, Cao M, Xu Q, Zhu J. Electroless nickel plating on silicon carbide nanoparticles, Surf. Coat.Technol., 172, 90 (2003). https://doi.org/10.1016/S0257-8972(03)00320-7.

[25] Ted Guo ML, Tsao CYA. Tribological behavior of aluminum/SiC/nickel-coated graphite hybrid composites, Mater. Sci. Eng.: A, 333, 134 (2002). https://doi.org/10.1016/S0921-5093(01)01817-2.

[26] Li F, Yan F, Yu L, Liu W. The tribological behaviors of copper-coated graphite filled PTFE composites, Wear, 237, 33 (2000). https://doi.org/10.1016/S0043-1648(99)00303-8.

[27] Mandal D, Dutta B K, Panigrahi S C. Wear properties of copper-coated short steel fiber reinforced stir cast Al–2Mg alloy composites, Wear, 265, 930 (2008). https://doi.org/10.1016/j.wear.2008.02.001.

[28] Miguel FL, Müller R, Rosenkranz A, Mathur S, Mücklich F. Analysis and modelling of the dry-sliding friction and wear behaviour of electrodeposited Ni and Ni-matrix-nanocomposite films, Wear,

346-347, 87 (2016). https://doi.org/10.1016/j.wear.2015.11.006.
[29] Popoola API, Loto CA, Osifuye CO, Aigbodion VS, Popoola OM. Corrosion and wear properties of Ni-Sn-P ternary deposits on mild steel via electroless method, Alexandria Eng. J.. 55, 2901 (2016) https://doi.org/10.1016/j.aej.2016.06.018.
[30] Wang W., Liu X, Liu K. Surface observations of a powder layer during the damage process under particulate lubrication. Wear, 297, 841 (2013). https://doi.org/10.1016/j.wear.2012.10.020.
[31] Xu Y, Zheng X, Hu X, Yin Y, Lei T. Preparation of the electroless Ni-P and Ni-Cu-P coatings on engine cylinder and their tribological behaviors under bio-oil lubricated conditions. Surf. Coat. Technol. 258, 790 (2014). https://doi.org/10.1016/j.surfcoat.2014.07.079.
[32] Deng X, Shi X, Liu X, Huang Y, Yan Z, Yang K, Wang Y. Effect of Ti_3SiC_2 on tribological properties of M50 matrix self-lubricating composites from 25 to 450°C. J. Mater. Eng. Perform. 4, 4595 (2017). https://doi: 10.1007/s11665-017-2908-z.